Amino Acids (2010) 38:1131–1143
DOI 10.1007/s00726-009-0323-y

ORIGINAL ARTICLE

Mass spectrometrical characterisation of mouse and rat synapsin isoforms 2a and 2b

Sung Ung Kang · Ming Zhang · Miguel Burgos · Gert Lubec

Received: 29 June 2009 / Accepted: 30 June 2009 / Published online: 16 July 2009

Abstract Synapsin 2 proteins are key elements of the synaptic machinery and still hold the centre stage in neuroscience research. Although fully sequenced at the nucleic acid level in mouse and rat, structural information on amino acid sequences and post-translational modifications (PTMs) is limited. Knowledge on protein sequences and PTMs, however, is mandatory for several purposes including conformational studies and the generation of antibodies. Hippocampal proteins from rat and mouse were extracted, run on two-dimensional gel electrophoresis and multi-enzyme digestion was carried out to generate peptides for mass spectrometrical analysis [nano-LC-ESI-(CID/ETD)-MS/MS]. As much as 12 synapsin 2 proteins (6 alpha and 6 beta isoforms) in the mouse and 13 synapsin 2 proteins (6 alpha and 7 beta isoforms) were observed in the rat. Protein sequences were highly identical to nucleic acid sequences, and only few amino acid exchanges probably representing polymorphisms or sequence conflicts were detected. Mouse and rat synapsins 2a differed in three amino acids, while rat and mouse synapsins 2b differed in two amino acids. As much as 13 phosphorylation sites were determined by MS/MS data in rat and mouse hippocampus and 5 were verified by phosphatase treatment. These findings are important for interpretation of previous results and design of future studies on synapsins.

Keywords Amino acid substitutions · Multi-enzyme digestion · Synapsin 2 isoforms · Synapsin phosphorylation · Two-dimensional gel electrophoresis

Introduction

Synapsins are key elements of the central nervous system with non-redundant functions. They play a major role in the synaptic machinery including exocytosis by controlling synaptic vesicles and therefore modulate neural transmission (Ferreira and Rapoport 2002; Hilfiker et al. 1999). The structure and function of synapsin 2 isoforms 2a and 2b have been reported (Hosaka and Sudhof 1998b).

Synapsin 2, with known isoforms 2a and 2b, is a member of the highly conserved synapsin family, shows several functional domains and is highly abundant in virtually all presynaptic nerve terminals (Hosaka and Sudhof 1998a, b; Sudhof 1989). Synapsins are bound to cytoskeletal elements, thus preventing release of neurotransmitters; but at synaptic activity, synapsins are phosphorylated and dissociate from synaptic vesicles that subsequently move to and fuse with the plasma membrane. Deletion of synapsins 1 and 2 altered the size of the vesicular pools (Lonart and Simsek-Duran 2006), decreased vesicular transport of specific neurotransmitters (Bogen et al. 2006) and regulated the use-dependent synaptic plasticity in the calyx of Held (Sun et al. 2006).

Hosaka et al. (1999) proposed a phospho-switch, controlling the dynamic association of synapsins with synaptic vesicles. The authors demonstrated that synapsin phosphorylation in the highly conserved A domain dissociated

Sung Ung Kang and Ming Zhang have contributed equally to this work.

Electronic supplementary material The online version of this article (doi:10.1007/s00726-009-0323-y) contains supplementary material, which is available to authorized users.

S. U. Kang · M. Zhang · M. Burgos · G. Lubec (✉)
Department of Pediatrics, Medical University of Vienna, Waehringer Guertel 18, 1090 Vienna, Austria
e-mail: gert.lubec@meduniwien.ac.at

synapsins from synaptic vesicles and modulated the binding of membrane phospholipids. From then, a series of synapsin phosphorylations were reported and reviewed in PhosphoSitePlus™; specific roles for these modifications have been suggested therein[1]: http://www.phosphosite.org/proteinAction.do?id=2386&showAllSites=true

Knowledge on protein sequences and post-translational modifications (PTMs), however, is mandatory and a prerequisite for the generation of specific antibodies, design of future functional and conformational studies, as well as understanding previous work on synapsins. Nucleic acid sequences may not provide sufficient information, in particular, for conformational predictions, as PTMs may alter protein structure and function significantly. This formed the rationale for carrying out the present study and it was the aim to investigate synapsin 2 isoforms in mouse and rat by determination of protein sequences and phosphorylations by a gel-based mass spectrometric approach.

Indeed, a series of mouse and rat synapsin 2 isoform sequences with an MS/MS sequence coverage between 90 and 99% including all C-termini and splicing sites were determined. In addition, several phosphorylation sites, of which some have been so far only predicted, were verified or confirmed herein.

Materials and methods

Animals

A total of 12 male C57/6JHim mouse littermates and 12 male Sprague-Dawley rat littermates, 10 weeks of age were used. The animals were housed in standard transparent laboratory cages in a temperature-controlled colony room (22°C). They were bred and kept at a 12 h/12 h light–dark cycle and had free access to food and water. Experiments were carried out under the licence of the Federal Ministry of Education, Science and Culture, which includes an ethical evaluation of the project. Animals were killed by neck dislocation, and the hippocampi were dissected within 1 min on dry ice and stored at −80°C.

Sample preparation

Hippocampal tissues were powdered and resuspended in 1.0 ml of sample buffer consisting of 7 M urea (Merck, Darmstadt, Germany), 2 M thiourea (Sigma, St Louis, MO, USA), 4% 3-[(3-cholamidopropyl) dimethylammonio]-1-propane-sulfonate (Sigma), 65 mM 1,4-dithioerythritol (DTT; Merck, Germany), 1 mM ethylenediaminetetraacetic acid (Merck), protease inhibitors complete® (Roche Diagnostics, Basel, Switzerland) and 1 mM phenylmethylsulfonyl chloride. The suspension was sonicated for 15 s, and the homogenised samples were kept at 22°C for 1 h and centrifuged at 14,000×*g* for 1 h. The supernatant was transferred into Ultrafree-4 centrifugal filter units (Millipore, Bedford, MA, USA) for desalting and concentrating proteins. The protein content was determined by the Bradford protein assay method.

Two-dimensional gel electrophoresis

Samples of 700 µg of protein extracts from each animal were loaded to 18 cm and immobilised at pH 3–10 with nonlinear gradient strips (GE Healthcare, USA). Focusing was started at the voltage of 200 V and then gradually increased to 8,000 V for 31 h and kept constant for a further 3 h. After the first dimension, the strips were equilibrated with 2% DTT for 15 min and then with 2.5% iodoacetamide for 15 min. After equilibration, the strips were loaded onto 9–16% gradient SDS-PAGE gels for two-dimensional separation. The gels were run at 45 mA per gel for 7 h. After that, the gels were fixed for 18 h in 50% methanol, containing 10% acetic acid and then stained with colloidal Coomassie Blue (Novex, San Diego, CA, USA) for 12 h on a rocking shaker. The molecular masses were determined by running standard protein markers (Bio-Rad Laboratories, Hercules, CA, USA) covering the range 10–250 kDa. Excess dye was washed from the gels with distilled water, and the gels were scanned with the ImageScanner (Amersham Bioscience).

In-gel multi-enzyme proteolysis

The synapsin 2 spots of interest were picked manually and were washed with 50% 50 mM ammonium bicarbonate/50% acetonitrile for 30 min two times; the washing solution was discarded at the end of each step. Subsequently, 100% acetonitrile was added to cover each gel piece and incubated for 5 min. The gel pieces were dried completely in a Speed-Vac Concentrator 5301 (Eppendorf, Germany).

The dried gel pieces were re-swollen with (1) 12.5 ng/µl trypsin (Promega, Madison, WI, USA) or (2) 25 ng/µl Asp-N (sequencing grade, Roche Diagnostic, Mannheim, Germany) or (3) 12.5 ng/µl Arg-C (Sigma, Steinheim, Germany) in digestion buffer consisting of 25 mM ammonium bicarbonate and incubated for 16 h at 37°C. In addition, (4) chymotrypsin (Roche, Germany) digestion was performed by adding 25 mM ammonium bicarbonate containing 12.5 ng/µl chymotrypsin (sequencing grade; Roche Diagnostic, Basel, Switzerland) and incubated for 16 h at 25°C. The supernatants were transferred to new 0.6 ml tubes and peptides were extracted with 30 µl 0.5%

[1] A series of authors with major contributions are listed in this link, but are not cited in the text of this manuscript.

formic acid/20% acetonitrile for 20 min in a sonication bath. This step was repeated once. Extracted buffers were pooled into the 0.6 ml tube and evaporated in a speedvac. The volume was reduced to 10 µl and another 10 µl HPLC-grade water was added.

In a further step, (5) gel pieces were covered with 30 µl of 10 ng/µl subtilisin (proteinase from *Bacillus subtilis* var. *biotecus* A, Sigma) in a digestion buffer consisting of a final concentration of 5.4 M urea and 0.1 M Tris, pH 8.5, and rehydrated for 10 min at 4°C. The supernatant was removed and replaced by 50 mM ammonium bicarbonate. Gel pieces were incubated for 1 h at 37°C. The reaction was stopped by the addition of 10% formic acid (a final concentration of 1% formic acid). The supernatant was transferred to 0.6 ml tubes. The peptides were extracted by adding 20 µl of 5% FA, followed by 20 min of sonication. This step was repeated once. The extracted peptides were subsequently analysed by nano-LC-ESI-qQTOF-MS/MS (qQTOF) and/or nano-LC-ESI-(CID/ETD)-MS/MS (high-capacity ion trap, HCT).

Phosphatase treatment

Selected synapsin 2 spots were washed and dried as given above and subsequently gel plugs were incubated in a solution of 0.5 µl of calf intestine alkaline phosphatase (New England Biolabs, Ipswich, MA, USA) in the presence of 100 mM ammonium bicarbonate for 1 h at 37°C. Thereafter, chymotrypsin was used for generation of peptides for mass spectrometric analysis that were subsequently analysed by LC-ESI-ion trap/MS.

Nano-LC-ESI-qQTOF-MS/MS (qQTOF)

The peptide solutions generated from multi-enzyme proteolysis were separated by UltiMate 3000 system (Dionex Corporation, Sunnyvale, CA, USA) equipped with a reversed phase PepMap C-18 analytic column (75 µm × 150 mm) and then identified by the qQTOF (Applied Biosystems, Foster City, CA, USA). Chromatography was performed using a mixture of two solutions, A (0.1% formic acid) and B (80% acetonitrile/0.85% formic acid), with a flow rate of 300 nl/min. First, a linear gradient between 4 and 60% B was run over 45 min, then 90% B was used for 5 min and 0% B for 25 min. Peptides eluted from the LC system were electrosprayed into the qQTOF. Each cycle consisted of one full scan mass spectrum (m/z 350–1,300), followed by MS/MS spectra of the three most abundant peptide ions in the full MS scan (m/z 50–1,300). The derived MS/MS data sets were converted to MASCOT generic format flat files (MGF files) by the AnalystQS 1.1 software (Applied Biosystems).

Nano-LC-ESI-(CID/ETD)-MS/MS (HCT)

The majority of extracted peptides were analysed by HCT. The HPLC was a biocompatible Ultimate 3000 system (Dionex Corporation, Sunnyvale, CA, USA) equipped with a Pep-Map100 C-18 trap column (300 µm × 5 mm) and PepMap100 C-18 analytic column (75 µm × 150 mm). The gradient was 4–30% B from 0 to 105 min, 80% B from 105 to 110 min, 4% B from 110 to 125 min (A means 0.1% formic acid; B means 0.08% formic acid in acetonitrile). The flow rate was 300 nl/min from 0 to 12 min, 75 nl/min from 12 to 105 min, and 300 nl/min from 105 to 125 min. The eluted peptides were electrosprayed and analysed by the HCT ultra-PTM discover system (Bruker Daltonics, Bremen, Germany), which records peptide spectra over the mass range of m/z 350–1,500, and MS/MS spectra in information-dependent data acquisition over the mass

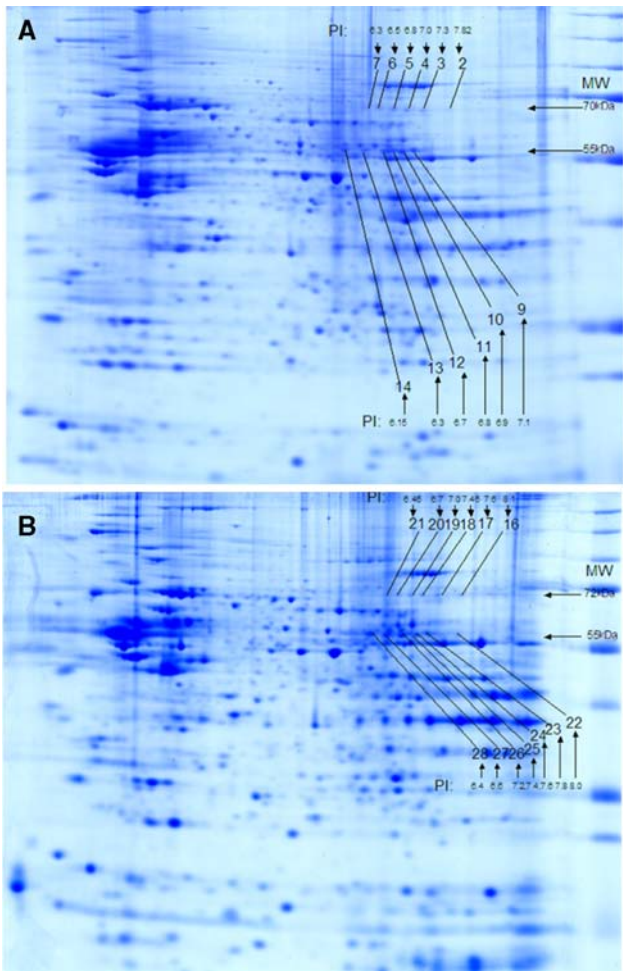

Fig. 1 Separation of mouse and rat synapsin 2 isoforms in two-dimensional gel. **a** The pattern of mouse synapsin 2 isoforms (2a; *spots 2–7* and 2b; *spots 9–14*) and **b** rat synapsin 2 isoforms (2a; *spots 16–21* and 2b; *spots 22–28*) in two-dimensional gel were shown with experimental pI value and molecular weight (MW) on each spot

range of m/z 100–2,800. Repeatedly, MS spectra were recorded followed by three data-dependent CID MS/MS spectra and three ETD MS/MS spectra, generated from the three highest intensity precursor ions. An active exclusion of 0.4 min after two spectra was used to detect low-abundance peptides. The collision energy was set automatically according to the mass and charge state of the peptides chosen for fragmentation. Multiple charged peptides were chosen for MS/MS experiments due to their good fragmentation characteristics. MS/MS spectra were interpreted, peak lists were generated and MGF files were obtained by the software of DataAnalysis 3.4 (Bruker Daltonics, Bremen, Germany).

Database searching

MASCOT generic format flat files were searched with the software of MASCOT v2.2 (Matrix Science, London, UK) against the latest NCBI database for protein identification. Searching parameters were set as follows: enzyme selected as trypsin, chymotrypsin, Asp-N and Arg-C with a maximum of two missing cleavage sites, limited to mouse or rat; a mass tolerance of 0.2 Da for peptide tolerance, 0.2 Da for MS/MS tolerance; fixed modification of carbamidomethyl(C) and variable modifications were selected as acetylation (K), deamidation (N, Q), methylation (C, D, E, H, K, N, Q, R, S, T) and phosphorylation (S, T, Y). The ion

Table 1 Sequence coverage of synapsin 2 isoforms by MS/MS depending on enzymes

Protein name	Total sequence coverage (%)[a]	Spot no.[b]	Theor. M.W. (kDa)[c]	Theor. pI[c]	Observ. M.W. (kDa)[d]	Observ. pI[d]	Combined sequence coverage (%)[e]	Trypsin (%)	Chymotrypsin (%)	Asp-N (%)	Arg-C (%)	Subtilisin (%)
Syn 2a_Rat	99	16	64	8.6	72	8.1	95	66	51	22	18	38
		17	64	8.6	72	7.6	94	57	48	20	17	32
		18	64	8.6	72	7.5	94	59	50	21	20	33
		19	64	8.6	72	7.0	96	73	51	19	19	30
		20	64	8.6	72	6.7	94	49	47	17	21	32
		21	64	8.6	72	6.5	93	57	46	23	19	28
Syn 2b_Rat	100	22	53	7.6	55	8.0	93	61	44	20	16	31
		23	53	7.6	55	7.8	93	62	48	20	16	29
		24	53	7.6	55	7.6	91	58	43	20	15	33
		25	53	7.6	55	7.4	98	79	63	22	23	30
		26	53	7.6	55	7.2	96	71	57	30	27	32
		27	53	7.6	55	6.6	97	73	56	19	20	28
		28	53	7.6	55	6.4	96	73	53	21	20	39
Syn 2a_Mouse	94	2	64	8.6	70	7.8	91	68	50	17	16	32
		3	64	8.6	70	7.3	90	68	51	17	17	34
		4	64	8.6	70	7.0	92	70	53	12	14	38
		5	64	8.6	70	6.8	91	69	52	21	19	28
		6	64	8.6	70	6.5	91	68	53	19	20	31
		7	64	8.6	70	6.3	92	73	48	14	15	29
Syn 2b_Mouse	100	9	53	7.6	55	7.1	95	71	62	18	17	33
		10	53	7.6	55	6.9	99	81	69	32	25	30
		11	53	7.6	55	6.8	96	78	66	20	19	32
		12	53	7.6	55	6.7	98	77	62	16	19	28
		13	53	7.6	55	6.3	90	71	50	19	21	31
		14	53	7.6	55	6.2	94	73	54	20	20	28

[a] Denotes sum up of identified peptides of each syn 2 isoform by MS/MS analysis [16–21 (syn 2a_Rat); 22–28 (syn 2b_Rat); 2–7 (syn 2a_Mouse); 9–14 (syn 2b_Mouse)]

[b] Spot number on two-dimensional electrophoresis gel

[c] Theoretical molecular weight and pI value of synapsin 2 isoforms

[d] Observed molecular weight and pI value of synapsin 2 isoforms on two-dimensional electrophoresis gel

[e] Denotes sum up of identified peptides of each spot with multi-enzymes

charge states were set as 1+, 2+ and 3+. Error-tolerant search was done to detect unspecific cleavage and unassigned modifications.

In parallel, MGF files were loaded to the software Modiro™ v1.1 (Protagen AG, Germany) to compensate and verify the translation of MS/MS spectra. Enzymes were selected as trypsin, chymotrypsin, Asp-N and Arg-C. Missing cleavage was set as two. Modifications were selected as oxidation (M) and carbamidomethyl (C). PTM explore strategies were selected as acetylation (K), deamidation (N, Q), methylation (C, D, E, H, K, N, Q, R, S, T) and phosphorylation (S, T, Y). Unknown mass shift and amino acid substitution were also included. Only results with significance higher than 90 scores were used.

Results

Six synapsin 2a isoforms and six synapsin 2b isoforms were observed in mouse hippocampus and six synapsin 2a isoforms (Fig. 1a) and seven synapsin 2b in the rat hippocampus (Fig. 1b). Only these well-separated spots representing synapsins 2, given above, were used for further studies.

Unambiguous mass spectrometric identification of synapsins 2 and sequence coverages are given in Table 1. Multi-enzyme digestion resulted in sequence coverage from 90 to 99% and individual results following digestion with the individual enzymes is shown in Table 1. All carboxy termini were identified, thus enabling determination of isoforms a and b.

The list of identified peptides is provided in Supplementary Table 1 and unidentified parts of the sequences are shown in Supplementary Figure 1.

The alignment of synapsin isoforms a and b in mouse and rat is illustrated in Fig. 2, revealing high identity between littermates of these rodents.

The splicing site distinguishing synapsin 2 isoforms a and b in mouse and rat (G458) is shown in Table 2.

Comparison between mouse and rat synapsins 2 is provided in Table 3: seven amino acids (sites at 42, 455, 486, 509, 511, 512, 513) were different between mouse and rat synapsins 2a. Two amino acids (sites at 42 and 455) were different between mouse and rat synapsins 2b.

Five amino acid substitutions observed in the individual spots are given in Table 4 and the corresponding spectra are given in Supplementary Figure 2.

Phosphorylation sites observed were partially confirmatory in nature; 13 phosphorylation sites were detected and 5 were verified by phosphatase treatment (Table 5). The corresponding spectra of phosphatase-treated synapsins are given in Fig. 3.

Additional modifications representing PTMs (as e.g. glycosylation of N339 in synapsin 2b in the rat) or modifications probably representing artifacts are shown in Table 6.

The detailed list of modified peptides is provided in Supplementary Table 2.

Discussion

Although sequence information at the nucleic acid level is known for synapsins 2a and 2b, only limited data are

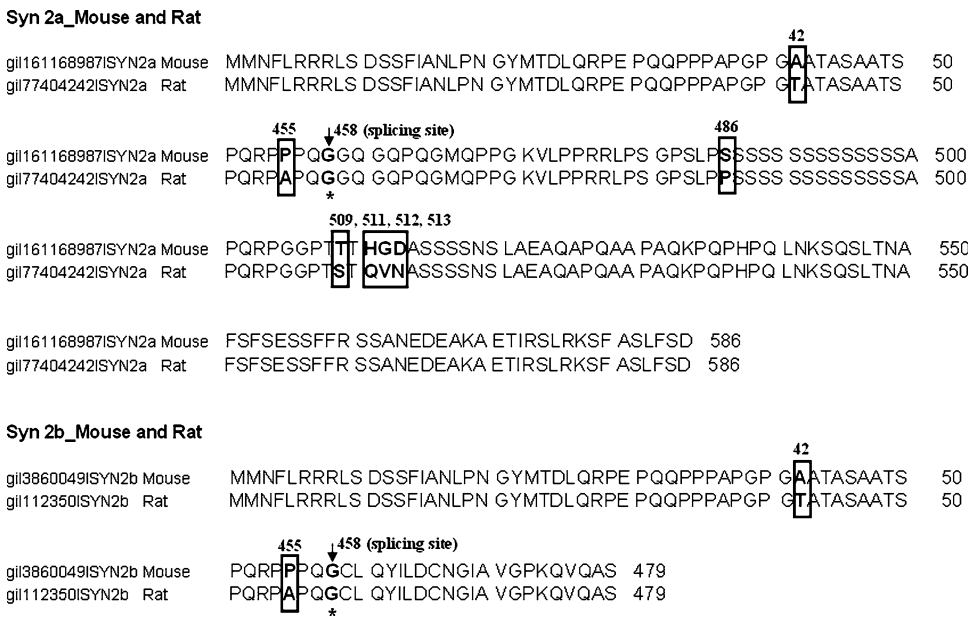

Fig. 2 Protein sequence alignment of synapsin 2 isoforms based on NCBI protein database between mouse and rat. It showed seven different amino acids (*site at 42, 455, 486, 509, 511, 512, 513*) in synapsin 2a and two different amino acids (*site at 42 and 455*) in synapsin 2b

Table 2 Identified peptides list from synapsin 2 splicing site (G458) by MS/MS analysis

Protein name	Spot no.	Method	Enzyme	Residues	Peptide sequence	Ion score	Delta	Modiro score	Sign.	Error
Syn 2a_Rat	16	HCT	Trypsin	449–471	K.TPPQRPAPQ**G**GPGQPQGMQPPGK.V	35	−0.0663			
	17	HCT	Trypsin	451–471	P.PQRPAPQ**G**GPGQPQGMQPPGK.V			187	100	−0.1916
	18	qQTOF	Trypsin	449–471	K.TPPQRPAPQ**G**GPGQPQGMQPPGK.V	37	0.0636			
	20	HCT	Trypsin	449–471	K.TPPQRPAPQ**G**GPGQPQGMQPPGK.V	45	−0.0310			
	21	qQTOF	Trypsin	449–471	K.TPPQRPAPQ**G**GPGQPQGMQPPGK.V			282	98.4	0.0091
Syn 2b_Rat	22	HCT	Trypsin	449–471	K.TPPQRPAPQ**G**CLQYILDCNGIAVGPK.Q	63	−0.0235			
	23	HCT	Trypsin	449–474	K.TPPQRPAPQ**G**CLQYILDCNGIAVGPK.Q	63	0.0125			
	25	HCT	Chymotrypsin	442–462	L.KEPDSSKTPPQRPAPQ**G**CLQY.I	12	0.0203			
	26	HCT	Asp-N	445–464	P.DSSKTPPQRPAPQ**G**CLQYIL.D	21	−0.1262			
	27	qQTOF	Chymotrypsin	442–462	L.KEPDSSKTPPQRPAPQ**G**CLQY.I	13	−0.0869			
	28	qQTOF	Chymotrypsin	442–462	L.KEPDSSKTPPQRPAPQ**G**CLQY.I	24	−0.0727			
Syn 2a_Mouse	2	HCT	Trypsin	449–471	K.TPPQRPPPQ**G**GPGQPQGMQPPGK.V	69	0.1007			
	4	HCT	Trypsin	449–471	K.TPPQRPPPQ**G**GPGQPQGMQPPGK.V	27	−0.0845			
	5	qQTOF	Trypsin	449–471	K.TPPQRPPPQ**G**GPGQPQGMQPPGK.V			307	100	−0.0857
	7	HCT	Trypsin	449–471	K.TPPQRPPPQ**G**GPGQPQGMQPPGK.V	44	0.1406			
	6	HCT	Trypsin	449–471	K.TPPQRPPPQ**G**GPGQPQGMQPPGK.V	27	−0.0350			
Syn 2b_Mouse	9	HCT	Trypsin	449–474	K.TPPQRPPPQ**G**CLQYILDCNGIAVGPK.Q	65	0.0171			
	10	HCT	Trypsin	449–474	K.TPPQRPPPQ**G**CLQYILDCNGIAVGPK.Q	36	−0.1305			
	11	HCT	Trypsin	449–474	K.TPPQRPPPQ**G**CLQYILDCNGIAVGPK.Q	21	−0.1588			
	12	qQTOF	Chymotrypsin	442–462	L.KEPDSSKTPPQRPPPQ**G**CLQY.I	29	−0.0759			
	14	qQTOF	Chymotrypsin	442–462	L.KEPDSSKTPPQRPPPQGCLQY.I	10	−0.0927			
	13	HCT	Subtilisin	442–461	L.KEPDSSKTPPQRPPPQ**G**CLQ.Y			278	100	−0.013

Mass spectrometrically identified amino acids of synapsin 2 isoforms between mouse and rat are marked with bold and underlined letters

Table 3 Distinction of synapsin 2 isoforms between rat and mouse by MS/MS analysis

Position	Protein name	Spot no.	Method	Enzyme	Residues	Peptide sequence	Ion score	Delta	Modiro score	Sign.	Error
(A) T42 from Syn 2 isoforms Rat and A42 from Mouse											
T42	Syn 2a_Rat	16	HCT	Subtilisin	26–43	D.LQRPEPQQPPPAPGPG**T**A.T	43	−0.0578			
		17	HCT	Subtilisin	27–43	L.QRPEPQQPPPAPGPG**T**A.T	33	0.1813			
		18	HCT	Subtilisin	26–43	D.LQRPEPQQPPPAPGPG**T**A.T	33	−0.1084			
		19	HCT	Subtilisin	26–43	D.LQRPEPQQPPPAPGPG**T**A.T	43	−0.1662			
		20	HCT	Trypsin	40–58	G.PG**T**ATASAATSAASPGPER.R	48	0.0387			
	Syn 2b_Rat	23	HCT	Subtilisin	26–43	D.LQRPEPQQPPPAPGPG**T**A.T	27	−0.1634			
		25	HCT	Subtilisin	26–43	D.LQRPEPQQPPPAPGPG**T**A.T	56	−0.1510			
		26	HCT	Subtilisin	26–44	D.LQRPEPQQPPPAPGPG**T**AT.A	48	−0.1311			
		27	HCT	Subtilisin	35–53	P.PPAPGPG**T**ATASAATSAAS.P	3	0.1293			
		28	qQTOF	Trypsin	42–58	G.**T**ATASAATSAASPGPER.R	50	−0.0885			
A42	Syn 2a_Mouse	4	HCT	Subtilisin	27–43	L.QRPEPQQPPPAPGPG**A**A.T	32	−0.1536			
		7	HCT	Subtilisin	26–43	D.LQRPEPQQPPPAPGPG**A**A.T			355	100	−0.0861
		6	HCT	Subtilisin	27–43	L.QRPEPQQPPPAPGPG**A**A.T	30	0.0220			
	Syn 2b_Mouse	9	HCT	Subtilisin	41–53	P.G**A**ATASAATSAAS.P	4	0.1932			
		10	HCT	Subtilisin	26–43	D.LQRPEPQQPPPAPGPG**A**A.T	52	0.0054			
		11	HCT	Subtilisin	26–43	D.LQRPEPQQPPPAPGPG**A**A.T	38	−0.0692			
		12	HCT	Trypsin	40–58	G.PG**A**ATASAATSAASPGPER.R	68	−0.1213			
		14	HCT	Trypsin	38–58	A.PGPG**A**ATASAATSAASPGPER.R	83	−0.0355			
(B) A455 from syn 2 isoforms Rat and P455 from Mouse											
A455	Syn 2a_Rat	16	HCT	Trypsin	449–471	K.TPPQRP**A**PQGGPGQPQGMQPPGK.V	35	−0.0663			
		17	HCT	Subtilisin	442–457	L.KEPDSSKTPPQRP**A**PQ.G	48	0.1645			
		18	qQTOF	Trypsin	449–471	K.TPPQRP**A**PQGGPGQPQGMQPPGK.V	37	0.0636			
		19	qQTOF	Chymotrypsin	442–457	L.KEPDSSKTPPQRP**A**PQ.G	44	0.0090			
		20	HCT	Subtilisin	442–457	L.KEPDSSKTPPQRP**A**PQ.G	58	0.1845			
		21	qQTOF	Trypsin	449–471	K.TPPQRP**A**PQGGPGQPQGMQPPGK.V			282	98.4	0.0091
	Syn 2b_Rat	22	HCT	Trypsin	449–471	K.TPPQRP**A**PQGCLQYILDCNGIAVGPK.Q	63	−0.0235			
		23	HCT	Trypsin	449–474	K.TPPQRP**A**PQGCLQYILDCNGIAVGPK.Q	63	0.0125			
		2	HCT	Asp-N	442–457	L.KEPDSSKTPPQRP**A**PQ.G			333	100	0.1222
		25	HCT	Chymotrypsin	442–462	L.KEPDSSKTPPQRP**A**PQGCLQY.I	12	0.0203			
		26	HCT	Asp-N	445–464	P.DSSKTPPQRP**A**PQGCLQYIL.D	21	−0.1262			
		27	qQTOF	Chymotrypsin	442–462	L.KEPDSSKTPPQRP**A**PQGCLQY.I	13	−0.0869			
		28	qQTOF	Chymotrypsin	442–462	L.KEPDSSKTPPQRP**A**PQGCLQY.I	24	−0.0727			

Table 3 continued

Position	Protein name	Spot no.	Method	Enzyme	Residues	Peptide sequence	Ion score	Delta	Modiro score	Sign.	Error
P455	Syn 2a_Mouse	2	HCT	Trypsin	449–471	K.TPPQRP**P**PQGGPGQPQGMQPPGK.V	69	0.1007			
		4	HCT	Trypsin	449–471	K.TPPQRP**P**PQGGPGQPQGMQPPGK.V	27	−0.0845			
		5	qQTOF	Trypsin	449–471	K.TPPQRP**P**PQGGPGQPQGMQPPGK.V			307	100	−0.0857
		7	HCT	Trypsin	449–471	K.TPPQRP**P**PQGGPGQPQGMQPPGK.V			184	99.8	0.1903
		6	HCT	Trypsin	449–471	K.TPPQRP**P**PQGGPGQPQGMQPPGK.V	27	−0.0350			
	Syn 2b_Mouse	9	HCT	Trypsin	449–474	K.TPPQRP**P**PQGCLQYILDCNGIAVGPK.Q			289	100	0.1923
		10	HCT	Trypsin	449–474	K.TPPQRP**P**PQGCLQYILDCNGIAVGPK.Q	36	−0.1305			
		11	HCT	Trypsin	449–474	K.TPPQRP**P**PQGCLQYILDCNGIAVGPK.Q	21	−0.1588			
		12	qQTOF	Chymotrypsin	442–462	L.KEPDSSKTPPQRP**P**PQGCLQY.I	29	−0.0759			
		14	qQTOF	Chymotrypsin	442–462	L.KEPDSSKTPPQRP**P**PQGCLQY.I	10	−0.0927			
		13	HCT	Subtilisin	442–461	L.KEPDSSKTPPQRP**P**PQGCLQ.Y			278	100	−0.013
(C) P486 from Syn 2a_Rat and S486 from Syn 2a_Mouse											
P486	Syn 2a_Rat	16	HCT	Trypsin	477–503	R.RLPSGPSLP**P**SSSSSSSSSSSSSAPQR.P	16	−0.1362			
		18	qQTOF	Trypsin	478–503	R.LPSGPSLP**P**SSSSSSSSSSSSSAPQR.P	48	0.0253			
		19	HCT	Trypsin	477–503	R.RLPSGPSLP**P**SSSSSSSSSSSSSAPQR.P	25	0.1803			
		20	HCT	Trypsin	477–503	R.RLPSGPSLP**P**SSSSSSSSSSSSSAPQR.P			197	91.7	0.029
		21	HCT	Trypsin	477–503	R.RLPSGPSLP**P**SSSSSSSSSSSSSAPQR.P	13	0.0459			
S486	Syn 2a_Mouse	2	HCT	Trypsin	477–503	R.RLPSGPSLP**S**SSSSSSSSSSSSSAPQR.P	57	−0.0140			
		4	HCT	Trypsin	477–503	R.RLPSGPSLP**S**SSSSSSSSSSSSSAPQR.P	25	−0.1988			
		5	HCT	Trypsin	477–503	R.RLPSGPSLP**S**SSSSSSSSSSSSSAPQR.P			345	100	0.0253
		7	HCT	Trypsin	477–503	R.RLPSGPSLP**S**SSSSSSSSSSSSSAPQR.P	54	−0.0005			
		6	HCT	Trypsin	477–503	R.RLPSGPSLP**S**SSSSSSSSSSSSSAPQR.P	64	−0.1481			

Mass spectrometrically identified amino acids of synapsin 2 isoforms between mouse and rat are marked with bold and underlined letters

Table 4 Identified amino acid substitutions in synapsin 2 isoforms from rat and mouse by MS/MS analysis

Protein name	Spot no.	Substitution sites	Method	Enzyme	Residues	Peptide sequence	Ion score	Error	Modiro score	Sign.	Error
Syn 2b_Rat	22	Ile → Asn 248	HCT	Trypsin	245–257	K.FPL**I**EQTYYPNHR.E	48	−0.1845			
	23	Phe → Val 191	HCT	Trypsin	188–200	R.QHA**F**GMAENEDFR.H	48	−0.0518			
	27	Phe → Val 191	HCT	Trypsin	188–200	R.QHA**F**GMAENEDFR.H	47	−0.1718			
	28	Gly → Trp 397	qQTOF	Asp-N	390–401	M.DCSMPLI**G**EHQV.E	35	0.1669			
Syn 2b_Mouse	12	Ile → Asn 220	HCT	Chymotrypsin	209–221	Y.AGLPSINSLES**I**Y.N			143	97.6	0.0126

Mass spectrometrically identified amino acids of synapsin 2 isoforms between mouse and rat are marked with bold and underlined letters

Table 5 Identified phosphorylation sites by MS/MS analysis

Protein name	Spot no.	Phosphorylated site	Residues	Peptide sequence[b]	Ion score	Error	Expect	Charge	Enzyme
Syn 2a_Rat	16	Phosphorylation S546	544–560	K.SQ**p**SLTNAFSFSESSFFR.S	89	0.0459	8.7E-08	2+	Trypsin
	19	Phosphorylation T422 S426	420–431	L.SR**p**TPAL**p**SPQRPL.T	13	−0.0738	65	2+	Chymotrypsin
	20	Phosphorylation S546	544–560	K.SQ**p**SLTNAFSFSESSFFR.S	105	0.0287	1.5E-08	2+	Trypsin
	20	Phosphorylation T422[a]	420–431	L.SR**p**TPALSPQRPL.T	35	−0.0282	0.38	2+	Chymotrypsin
Syn 2b_Rat	24	Phosphorylation T422	420–431	L.SRTPALSPQRPL.T	33	0.1325	0.24	2+	Chymotrypsin
	25	Phosphorylation S426[a]	420–431	L.SRTPAL**p**SPQRPL.T	35	−0.0458	0.041	2+	Chymotrypsin
	26	Phosphorylation T338[a]	337–345	W.K**p**TNTGSAML.E	11	−0.0784	72	2+	Chymotrypsin
	26	Phosphorylation S426[a]	420–431	L.SRTPAL**p**SPQRPL.T	51	−0.0579	0.0096	2+	Chymotrypsin
	26	Phosphorylation T422	420–431	L.SR**p**TPALSPQRPL.T	30	0.0157	37	2+	Subtilisin
	27	Phosphorylation S426[a]	420–431	L.SRTPAL**p**SPQRPL.T	43	−0.0675	0.056	2+	Chymotrypsin
	27	Phosphorylation S446	442–457	L.KEPD**p**SSKTPPQRPAPQ.G	39	0.1182	0.56	2+	Subtilisin
Syn 2a_Mouse	7	Phosphorylation S446	443–448	K.EPD**p**SSK.T	18	0.1892	1.4	1+	Trypsin
	3	Phosphorylation S446	443–448	K.EPD**p**SSK.T	12	0.0948	6.4	1+	Trypsin

[a] This phosphorylation site has been confirmed by phosphatase treatment

[b] **p**S or **p**T denotes phosphorylated serine or threonine

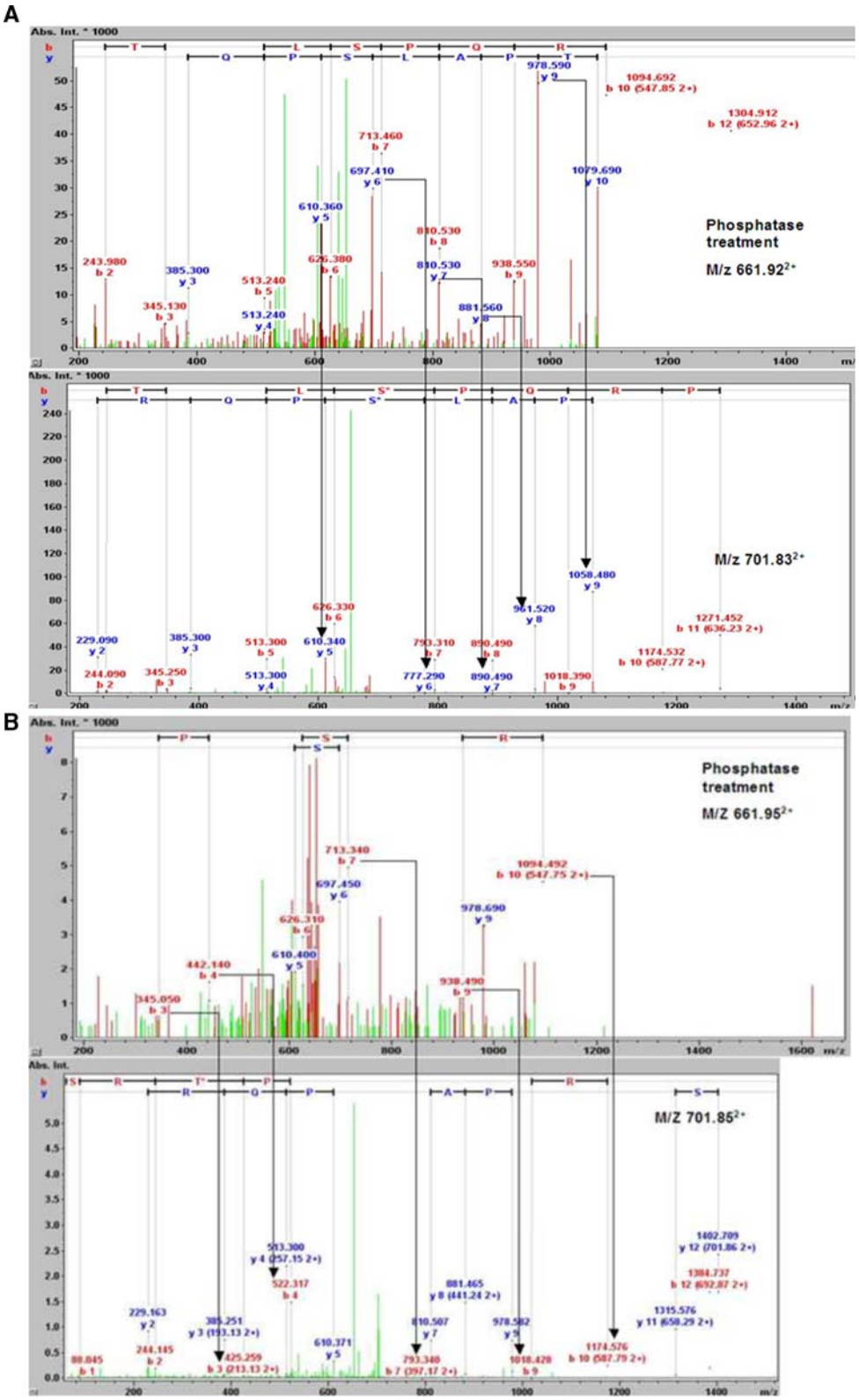

Fig. 3 Identification and verification of phosphorylated peptides with phosphatase treatment. **a** Phosphorylation at S426 (420SRTPALpSPQRPL431, m/z 661.922+) in sample 27 and **b** at T422 (420SRpTPALSPQRPL431, m/z 701.832+) in sample 20 demonstrated that 79.9 Da mass shift in each peptide after phosphatase treatment

Table 6 Identified protein modifications on synapsin 2 isoforms by MS/MS analysis

Protein name	Spot no.	Deamidation sites	Acetylation sites	Methylation sites	Glycosylation sites	Other modification sites
Syn 2a_Rat	16	Q73, N153, N171, N255, N339, N549	M2			Gln → pyro-Glu Q94, Q188, Q405
	17	Q73, N153, N171, N255, Q347, N416, N564	M1, M2	D390, E402, E403		Gln → pyro-Glu Q94, Q188, Q405
	18	Q69, N171, N255, Q457				Gln → pyro-Glu Q94, Q188, Q405
	19	Q167, Q250, N339	M2	S98, D103		Gln → pyro-Glu Q94, Q188, Q405
	20	N20, Q69, Q73, N153, N171, Q250, N255, N339, N549, N564				Gln → pyro-Glu Q94, Q188, Q405
	21	N20, Q69, Q73, Q146, Q153, N171, N255, N339, N457, N549, N564	M1	C361, S362, E363, D390, C391, S392, D403, R404		Gln → pyro-Glu Q94, Q188, Q405
Syn 2b_Rat	22	Q73, N171, N339, Q347, N457, N467	M1	D390, S392		Gln → pyro-Glu Q94, Q188, Q405
	23	Q73, Q90, N171, N339, Q437, N467	M1	E122		Gln → pyro-Glu Q94, Q188, Q405
	24	N20, N171, N467		E122		Gln → pyro-Glu Q94, Q188, Q405
	25	N20, N196, Q250, Q461, N467	M1		Hex(2)HexNAc(2)Pent(1) N339	Gln → pyro-Glu Q94, Q188, Q405
	26	N20, N171, N196, N467	M2			Gln → pyro-Glu Q188, Q405
	27	N3, N20, Q73, N171, Q250, N339, Q434, Q437, N467	M1, M2	E249, D390, C391, S392		Gln → pyro-Glu Q94, Q188, Q405
	28	N20, N171, Q250, N467	M1	E122		Gln → pyro-Glu Q94, Q188, Q405
Syn 2a_Mouse	2	N20, Q73, N153, Q250, Q347, N549		D126		Gln → pyro-Glu Q405
	3	N20, N196, Q250				Gln → pyro-Glu Q94, Q188, Q405
	4	N20, Q73, Q146, N153, N171, N196, N255, N339, Q462, N549		D390, C391, S392, E398, H399, Q400		Gln → pyro-Glu Q94, Q188, Q405
	5	N20, N171, N196, Q250, N339, Q347, Q435, N564	M1	E122, D390, C391, S392		Gln → pyro-Glu Q94, Q188, Q405
	6	Q73, N153, N171, N255, Q400, N549, R560	M1	E243, E249, D390, C391, S392		Gln → pyro-Glu Q94, Q188, Q405
	7	N20, Q73, N153, Q167, N171, N196, N255, N339, Q457, Q462, N549, N564				Gln → pyro-Glu Q94, Q188, Q405

Table 6 continued

Protein name	Spot no.	Deamidation sites	Acetylation sites	Methylation sites	Glycosylation sites	Other modification sites
Syn 2b_Mouse	9	Q73, N153, N255, Q435, Q457, N467	M1	E249, S362		Gln → pyro-Glu Q188, Q405
	10	N20, Q146, N196, Q250, N255, N339, Q347, Q428, Q434, N467	M1, M2	D121, E122, D390, C391, S392		Gln → pyro-Glu Q94, Q188, Q405, E258
	11	N20, N171, Q250, N255, Q434, N467		D121		Gln → pyro-Glu Q94, Q188, Q405, E258
	12	N20, Q69, Q73, N171, N196, Q250, N255, Q290, Q300, Q452, N467	M1	E122, E249		Gln → pyro-Glu Q94, Q188, Q405, E258
	13	N20, N171, N255, N339, Q347, N416, N467	M1	D121		Gln → pyro-Glu Q94, Q188, Q405
	14	N20, Q64, Q69, Q73, N153, N196, Q250, Q300, N339, Q347, Q00, Q434, Q456, N467	M1	E122, K244, E249, T340, C361, S362, E363, C391, E402, D403		Gln → pyro-Glu Q94, Q188, Q405

available at the protein level. As there is a long and unpredictable course from DNA/RNA to protein and PTMs, essential for structure and function, it cannot be predicted and determined from nucleic acid sequences. In the current study, indeed, high sequence coverage was obtained for synapsins 2a and 2b in mouse and rat, revealing the highest consensus between these species. In the case of comparing synapsins 2b between mouse and rat (100% of sequence coverage obtained for both species), the protein sequence determined showed 99.4% of identity. This reflects extraordinarily high sequence conservation between mouse and rat, and herein the data from the database at the nucleic acid level are confirmed.

There were, however, amino acid substitutions as revealed by analysing individual spots representing synapsin 2. While no amino acid substitutions were detected for six spots of mouse and six spots of rat synapsin 2a, four spots of 2b in rat and one spot of synapsin 2b in the mouse (Table 4, Supplementary Figure 2) showed substitutions. These amino acid substitutions may reflect mutations or polymorphisms and were revealed by MS/MS sequencing and data mining by Mascot and Modiro softwares based on mass shifts. The likelihood that an unknown modification was mimicking the mass shift for the amino acid substitutions is low because the Modiro software is designed to detect unknown mass shifts and, moreover, no parental/precursor ion was detectable. Polymorphisms for synapsins were reported and were linked to diseases of the CNS (Lachman et al. 2006). The protein structure determined allows generation of specific antibodies against several epitopes of mouse and rat synapsins 2, as well as synapsins 2 with amino acid substitutions. The functional relevance of the latter remains elusive, although the amino acid substitutions in the third domain, consisting of 308 amino acids, may interfere with binding to ATP, actin and synaptic vesicle proteins (PROSITE documentation PDOC00345). It remains open which and to what extent conformational changes result from the substitutions.

A series of synapsin 2a and 2b phosphorylations have been published in mouse and rat. As already reported, the phosphorylation sites were verified (Supplementary Table 2). Five phosphorylation sites were confirmed in rat synapsins 2a and 2b by phosphatase treatment (Table 2, Fig. 3). Phosphorylation on T338 in the C domain may affect ATP, actin and synaptic-protein binding, while phosphorylations T422 and S426 may modulate interactions with other proteins by the proline-rich region G (Hall et al. 1990). Again, this is of utmost relevance for the generation of antibodies against the corresponding phosphopeptides.

A series of modifications, including deamidations and methylations, to name a few, representing artifacts and glycosylation at N339 on synapsin 2b of the rat, is

proposed (Supplementary Figure 3). Glycosylation of synapsins is of functional relevance and may even affect phosphorylation (Cole and Hart 1999; Tallent et al. 2009).

Taken together, we provided high sequence coverage information on synapsins 2 in the mouse and rat, revealing highest identity between the two species. Amino acid substitutions and confirmation of phosphorylation sites may form the basis for functional and conformational studies, both, for interpretation of previous work and the design of future studies on synapsin 2. Moreover, the provided information generated by mass spectrometry (Ahmed et al. 2009; Gruber-Olipitz et al. 2006; John et al. 2008; Myung et al. 2008) may be of value for the design of sequence- and phosphorylation-specific antibodies.

References

Ahmed KE, Chen WQ, John JP et al (2009) Complete sequencing of the recombinant granulocyte-colony stimulating factor (filgrastim) and detection of biotinylation by mass spectrometry. Amino Acids (in press)

Bogen IL, Boulland JL, Mariussen E et al (2006) Absence of synapsin I and II is accompanied by decreases in vesicular transport of specific neurotransmitters. J Neurochem 96:1458–1466

Cole RN, Hart GW (1999) Glycosylation sites flank phosphorylation sites on synapsin I: O-linked N-acetylglucosamine residues are localized within domains mediating synapsin I interactions. J Neurochem 73:418–428

Ferreira A, Rapoport M (2002) The synapsins: beyond the regulation of neurotransmitter release. Cell Mol Life Sci 59:589–595

Gruber-Olipitz M, Yang JW, Slavc I, Lubec G (2006) Nectin-like molecule 1 is a high abundance protein in cerebellar neurons. Amino Acids 30:409–415

Hall FL, Mitchell JP, Vulliet PR (1990) Phosphorylation of synapsin I at a novel site by proline-directed protein kinase. J Biol Chem 265:6944–6948

Hilfiker S, Pieribone VA, Czernik AJ et al (1999) Synapsins as regulators of neurotransmitter release. Philos Trans R Soc Lond B Biol Sci 354:269–279

Hosaka M, Sudhof TC (1998a) Synapsin III, a novel synapsin with an unusual regulation by Ca^{2+}. J Biol Chem 273:13371–13374

Hosaka M, Sudhof TC (1998b) Synapsins I and II are ATP-binding proteins with differential Ca^{2+} regulation. J Biol Chem 273:1425–1429

Hosaka M, Hammer RE, Sudhof TC (1999) A phospho-switch controls the dynamic association of synapsins with synaptic vesicles. Neuron 24:377–387

John JP, Oh JE, Pollak A, Lubec G (2008) Identification and characterisation of arsenite (+3 Oxidation State) methyltransferase (AS3MT) in mouse neuroblastoma cell line N1E-115. Amino Acids 35:355–358

Lachman HM, Stopkova P, Papolos DF et al (2006) Analysis of synapsin III-196 promoter mutation in schizophrenia and bipolar disorder. Neuropsychobiology 53:57–62

Lonart G, Simsek-Duran F (2006) Deletion of synapsins I and II genes alters the size of vesicular pools and rabphilin phosphorylation. Brain Res 1107:42–51

Myung JK, Frischer T, Afjehi-Sadat L et al (2008) Mass spectrometrical analysis of the processed metastasis-inducing anterior gradient protein 2 homolog reveals 100% sequence coverage. Amino Acids 35:485–494

Sudhof TC (1989) Synaptic vesicles. Curr Opin Cell Biol 1:655–659

Sun J, Bronk P, Liu X et al (2006) Synapsins regulate use-dependent synaptic plasticity in the calyx of Held by a Ca^{2+}/calmodulin-dependent pathway. Proc Natl Acad Sci USA 103:2880–2885

Tallent MK, Varghis N, Skorobogatko Y et al (2009) In vivo modulation of O-GlcNAc levels regulates hippocampal synaptic plasticity through interplay with phosphorylation. J Biol Chem 284:174–181